Computational Spectroscopy of Carbon Monoxide Isotopomers in Helium Clusters†

Tatjana Škrbić,‡ Saverio Moroni,* and Stefano Baroni§

Scuola Internazionale Superiore di Studi Avanzati (SISSA) and CNR-INFM DEMOCRITOS National Simulation Center via Beirut 2-4, 34014 Trieste, Italy

Received: March 3, 2007; In Final Form: May 18, 2007

The rotational excitation spectrum, including the vibrational shift of the rotational band, of several CO isotopomers solvated in He clusters has been calculated. Reptation quantum Monte Carlo simulations are used in conjunction with an accurate He−CO potential energy surface, which quantitatively describes the rovibrational spectrum of the binary complex. Our simulations, when compared with number-selective infrared spectra taken for different isotopomers, help discriminate among the alternative assignments proposed for cluster sizes around 15 He atoms. The origin of the vibrational band has a red shift that is nearly linear with the cluster size within the first solvation shell and is almost constant up to the largest cluster studied, well beyond completion of the second solvation shell. A blue upturn at even larger sizes would be needed to attain the nanodroplet limit, as recently estimated from the isotopic dependence of the measured R(0) transitions.

I. Introduction

Recent years have witnessed an impressive progress in the study, both experimental and theoretical, of helium droplets and clusters doped with molecular impurities.[1−4] The introduction and rapid development of experimental techniques for size-selective spectroscopy,[5] in a range that now encompasses several tens of He atoms,[6,7] have provided a unique opportunity to directly compare theoretical results[8,9] against measurements. In this size range, much insight into the relationship between structural and dynamical properties and the onset of superfluidity has been gained by quantum Monte Carlo simulations using high-quality interparticle potentials. However, the increasing body of experimental information reveals a new and unexpectedly rich phenomenology, with details of the interaction between He atoms and molecular impurity playing a crucial role[10] and calling for a deeper investigation.

One of the most studied dopant molecules is carbon monoxide.[7,11−16] Whereas some of the main properties of the evolution of the observed spectra with the cluster size[11] are well understood,[13] further measurements with isotopical substitution of carbon and/or oxygen[7,12] reveal interesting features with possible implications on the assignment of spectral lines and pose new questions on the approach to the nanodroplet (large size) limit. The isotope effect has been used[16] to determine both the rotational constant and the shift of the origin of the vibrational band from the R(0) line measured in large droplets (thousands of He atoms). However, a similar analysis applied in the size range around 20 He atoms gives unexpectedly scattered results.[7]

In this paper we report on a quantum Monte Carlo study of both the rotational excitation spectrum and its vibrational shift in CO in He clusters ($CO@He_N$) with up to several tens of He atoms and consider all of the four CO isotopomers employed in the experimental studies.[7,11,12,16] We use a recent He−CO potential,[17] which quantitatively reproduces the known[18] rovibrational excitations of the binary complex, that includes, in particular, the vibrational shift. Our results support the "D numbering", one of various assignments for $N \approx 15$ proposed[7] as an alternative to the conventional numbering adopted in ref 11. We also discuss the approach to the nanodroplet regime. The calculated red shift of the vibrational band turns out to be stronger with two complete solvation shells than the estimate given for the nanodroplet limit.[16] Comparison with the R(0) transitions observed in the IR spectrum[7] suggests that for $N \gtrsim 30$ the red shift should be even larger than our result. This would require either a substantial blue upturn to eventually attain the nanodroplet value or a revision of the latter.

II. Theory

We employ a realistic model Hamiltonian in which N He atoms are treated as point-like particles, and the CO molecule is a rigid linear rotor. Interactions are described by pair potentials and are obtained from ab initio quantum chemistry calculations. For He−He we adopt the SAPT2 potential of Korona et al.,[19] whereas for He−CO we use the "CBS+corr" potential energy surface (PES) of Peterson and McBane,[17] which is supposed to be very accurate. We use the two-dimensional version of this PES, which is appropriate for the vibrational ground- and first excited-state of the molecule (V_{00} and V_{11}, respectively). In particular, the CBS+corr potential is known to give a value for the shift of the vibrational band in the He−CO binary complex in quantitative agreement with the experiment, whereas the SAPT PES[20] that we adopted in our previous study of this system[13] overestimates it by a factor of 2.

We use the reptation quantum Monte Carlo (RQMC) method[21] to calculate unbiased[22] estimates for the ground-state energy, structural properties, and imaginary-time correlation functions of the doped clusters.[8] Rotational energies are extracted from imaginary-time correlation functions via an inverse Laplace transform. Further details of our quantum Monte Carlo simulations can be found in ref 13.

The vibrational shift is defined as the difference between the rotational ground-state energies of the cluster corresponding to

† Part of the "Roger E. Miller Memorial Issue".

* To whom correspondence should be addressed. E-mail: moroni@democritos.it.

‡ E-mail: skrbic@sissa.it.

§ E-mail: baroni@sissa.it.

10.1021/jp071740y CCC: $37.00
Published on Web 07/12/2007

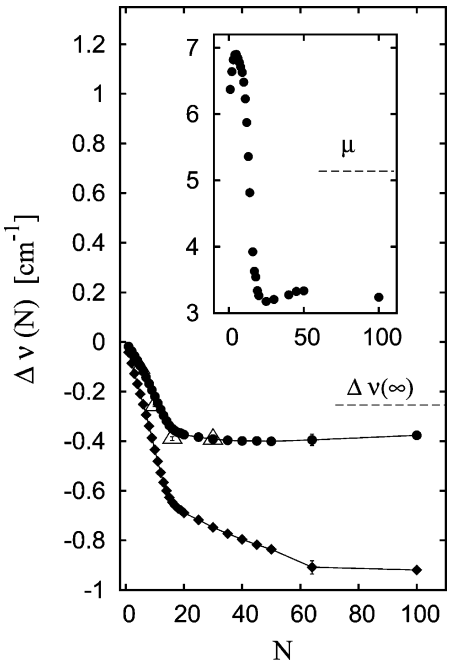

Figure 1. Vibrational shift of CO@He$_N$ clusters: pertubative estimates using the CBS+corr potential (filled circles) and the SAPT potential (filled diamonds), and complete calculations using the CBS+corr potential (open triangles). The dashed line is the nanodroplet limit according to ref 16. Inset: the "chemical potential", $\Delta E_N = -[E(N) - E(M)]/(N - M)$, with M being the largest available cluster size smaller than N. The horizontal dashed line is the bulk He chemical potential. For $N \geq 30$, the SAPT results are obtained from densities calculated with the CBS+corr potential (consistently with the perturbative approach).

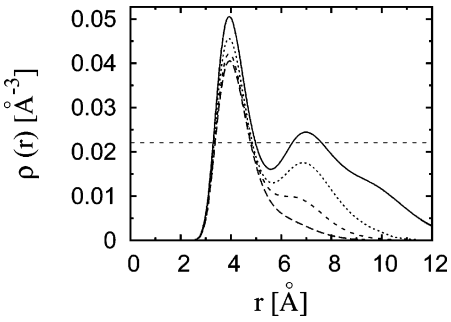

Figure 2. Radial density profiles of CO@He$_N$ clusters for $N = 20$, 30, 50, and 100. The horizontal line is the equilibrium density of bulk He.

the V_{00} and the V_{11} PES, which describe the interaction of He atoms with the molecule in its vibrational ground- and first excited-state, respectively. As this difference is small with respect to the individual energies, whose statistical uncertainties grow with the cluster size, we resort to a perturbative approach.[14] We thus evaluate the vibrational shift as the expectation value of $V_{00} - V_{11}$, sampled on the random walk generated with either PES. Comparison with complete, non-perturbative calculations, performed at selected cluster sizes up to $N = 30$, shows that this perturbative approach is accurate enough for the purposes of this work.

Different isotopomers are treated[16] by using the appropriate values of the mass and gas-phase rotational constant and by shifting the potential along the molecular axis by an amount (ζ) opposite to the shift in the center of mass with respect to the reference isotopomer, $^{12}C^{16}O$. In the two-dimensional PES approximation, this implies neglecting a small effect on the potential due to the change in the vibrational ground state of the molecule upon isotopic substitution. Using correlated sampling to infer the properties of all the isotopomers from configurations sampled for one of them is, in principle, straightforward within RQMC.[21] In practice, however, we have found very large fluctuations of the weights, and the results presented here are obtained with independent simulations for different isotopomers.

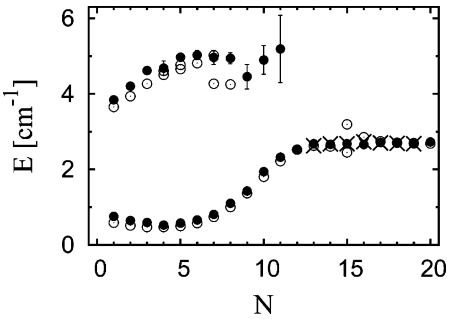

Figure 3. Rotational energies of $^{13}C^{18}O@He_N$ clusters: RQMC calculations (filled circles) and experiment[7] (open circles, conventional numbering; crosses, weighted average of the line positions with the D numbering). The experimental values are obtained from the measured R(0) line by subtracting the origin of the band in the gas-phase and the calculated vibrational shift.

III. Results

A. Vibrational Shift. Our results for the vibrational shift $\Delta\nu(N)$, together with a few direct, non-perturbative estimates at selected N values, are shown in Figure 1The difference between the two estimates is largest around $N = 20$, possibly in relation to the change in the behavior of the chemical potential at this cluster size (shown in the inset). The N dependence of the vibrational shift is qualitatively similar to that computed[14] using the SAPT PES of Heijmen et al.,[20] with an almost linear behavior within the first solvation shell, and a significant change in the slope between $N = 15$ and $N = 20$. However there are quantitative differences, whose importance for the agreement of the calculated R(0) transitions with the available experimental information will be discussed in Section IIID Using the CBS+corr potential, the initial slope closely matches the value measured[18] for the binary complex, and the red shift saturates around $N = 50$, with a weak upturn at larger sizes. With the SAPT potential the initial slope is twice as large, and the saturation of the red shift drifts to larger sizes and it appears to be monotonic, at least in the range studied here.

The estimated[16] nanodroplet limit is much closer to the CBS+corr result. On the other hand, the analytic expression of this potential is fitted to a PES calculated for distances up to 7.9 Å.[17] From the extension of radial density profiles, shown in Figure 2, we see that already for $N = 30$ the calculation relies on extrapolation. In particular, the CBS+corr difference $V_{11}(R,\theta) - V_{00}(R,\theta)$ is positive for most values of θ at $R \gtrsim 7$Å, with an unphysical persistence of a significant angular dependence at large distance. This explains the blue upturn of the CBS+corr vibrational shift, but it casts doubts on its accuracy at large sizes. In particular, the tendency seen in Figure 1 to approach the estimated nanodroplet limit[16] is possibly due to a deficiency of the potential at large distances. The SAPT method, instead, directly determines the dispersion coefficients, thus affording a better accuracy at large distances. It yields a negative value for $V_{11}(R,\theta) - V_{00}(R,\theta)$, with a weak nearly quadrupolar angular dependence (except, of course, close to the molecule). Including the rotational excitations we can directly compare with the measured R(0) transitions. We will see in Section IIID that

TABLE 1: The a-Type Rotational Energies (E_{rot}, in K) of CO@He$_N$ and Their Spectral Weights (A)[a]

	CBS+corr								SAPT	
	$^{12}C^{16}O$		$^{13}C^{16}O$		$^{12}C^{18}O$		$^{13}C^{18}O$		$^{12}C^{16}O$	
N	E_{rot}	A	E_{rot}	A	E_{rot}	A	E_{rot}	A	E_{rot}	A
1	0.99(18)	0.113(16)	0.9(3)	0.11(3)	0.68(19)	0.096(15)	1.09(8)	0.143(9)	0.79(4)	0.112(4)
2	0.96(7)	0.223(12)	0.94(8)	0.231(14)	0.73(16)	0.21(2)	0.93(4)	0.251(8)	0.67(6)	0.196(11)
3	0.84(5)	0.281(13)	0.87(3)	0.316(6)	0.81(4)	0.313(8)	0.85(2)	0.337(6)	0.768(18)	0.292(4)
4	0.83(6)	0.352(13)	0.75(11)	0.35(3)	0.79(6)	0.376(16)	0.75(6)	0.378(15)	0.874(12)	0.367(3)
5	0.92(2)	0.410(6)	0.87(3)	0.414(9)	0.89(3)	0.429(8)	0.83(2)	0.431(6)	0.991(12)	0.411(4)
6	1.03(4)	0.431(10)	1.02(3)	0.446(9)	1.00(4)	0.452(12)	0.95(3)	0.458(8)	1.149(11)	0.448(4)
7	1.29(3)	0.452(8)	1.24(3)	0.467(8)	1.20(3)	0.466(9)	1.16(4)	0.478(14)	1.408(19)	0.463(7)
8	1.69(3)	0.473(9)	1.67(2)	0.494(7)	1.62(4)	0.489(13)	1.58(4)	0.511(13)	1.87(3)	0.482(10)
9	2.24(7)	0.50(2)	2.14(8)	0.50(3)	2.11(8)	0.51(3)	2.05(9)	0.52(4)	2.47(5)	0.536(19)
10	3.00(7)	0.62(3)	2.85(6)	0.61(3)	2.87(7)	0.64(3)	2.79(8)	0.66(4)	3.49(15)	0.57(4)
11	3.56(5)	0.74(3)	3.53(6)	0.78(4)	3.45(5)	0.78(3)	3.34(9)	0.79(6)	3.84(3)	0.60(5)
12	4.01(3)	0.880(9)	3.85(9)	0.849(5)	3.86(2)	0.913(9)	3.64(10)	0.86(7)	4.07(9)	0.87(5)
13	4.16(4)	0.911(16)	4.05(3)	0.925(9)	3.991(14)	0.941(4)	3.85(2)	0.942(7)	4.26(5)	0.931(11)
14	4.23(2)	0.935(4)	4.08(3)	0.936(8)	4.00(2)	0.943(4)	3.83(2)	0.939(6)	4.37(3)	0.87(5)
15	4.299(10)	0.949(2)	4.13(2)	0.937(15)	4.01(2)	0.943(5)	3.85(3)	0.923(12)	4.26(4)	0.931(7)
16	4.307(13)	0.950(3)	4.19(2)	0.957(4)	4.00(3)	0.941(9)	3.83(3)	0.938(8)	4.33(3)	0.947(5)
17	4.281(14)	0.946(3)	4.13(2)	0.946(5)	4.03(2)	0.952(3)	3.900(16)	0.953(3)	4.38(4)	0.950(8)
18	4.34(3)	0.958(5)	4.14(3)	0.948(6)	4.068(16)	0.954(3)	3.88(3)	0.947(7)	4.38(4)	0.951(8)
19	4.33(2)	0.955(3)	4.15(3)	0.951(4)	4.02(6)	0.947(11)	3.90(2)	0.954(4)	4.37(4)	0.953(7)
20	4.30(4)	0.950(7)	4.20(2)	0.957(4)	3.98(3)	0.940(6)	3.92(3)	0.956(5)	4.34(4)	0.949(7)
25	4.35(5)	0.963(6)							4.31(12)	0.956(12)
30	4.05(11)	0.89(4)							4.33(11)	0.961(8)
35	4.12(7)	0.92(2)								
40	4.14(7)	0.938(15)								
45	4.14(9)	0.94(2)								
50	4.15(10)	0.945(18)								
100	4.05(9)	0.943(11)								

[a] Computed with RQMC using the CBS+corr potential for four CO isotopomers[22,25] and with the SAPT potential for the normal isotopomer. The SAPT data at $N = 25$ and 30 are from ref 13.

TABLE 2: The b-Type Rotational Energies (E_{rot}, in K) of CO@He$_N$ and Their Spectral Weights (A)

	CBS+corr								SAPT	
	$^{12}C^{16}O$		$^{13}C^{16}O$		$^{12}C^{18}O$		$^{13}C^{18}O$		$^{12}C^{16}O$	
N	E_{rot}	A	E_{rot}	A	E_{rot}	A	E_{rot}	A	E_{rot}	A
1	5.88(20)	0.873(6)	5.58(23)	0.871(8)	5.37(14)	0.855(7)	5.52(5)	0.850(7)	5.85(4)	0.868(3)
2	6.44(13)	0.759(6)	6.22(16)	0.746(13)	5.8(3)	0.746(13)	6.05(8)	0.736(4)	5.9(3)	0.71(5)
3	6.88(17)	0.683(3)	6.80(8)	0.666(3)	6.65(12)	0.662(3)	6.64(8)	0.647(4)	6.67(10)	0.664(7)
4	7.2(3)	0.611(3)	6.7(5)	0.594(20)	7.1(3)	0.595(5)	6.7(3)	0.587(3)	7.41(10)	0.607(3)
5	7.75(12)	0.565(3)	7.41(18)	0.556(4)	7.51(18)	0.541(2)	7.15(14)	0.536(3)	7.70(9)	0.561(4)
6	7.7(3)	0.536(3)	7.54(20)	0.524(3)	7.5(2)	0.515(3)	7.23(17)	0.510(4)	7.99(11)	0.528(3)
7	7.62(15)	0.515(4)	7.54(17)	0.505(4)	7.33(17)	0.499(5)	7.1(3)	0.486(5)	7.86(13)	0.513(4)
8	7.41(13)	0.496(7)	7.38(12)	0.478(5)	7.12(20)	0.477(8)	7.11(20)	0.458(8)	7.50(17)	0.491(7)
9	7.0(3)	0.465(18)	6.8(4)	0.46(2)	6.7(3)	0.45(2)	6.4(5)	0.44(3)	7.4(2)	0.438(17)
10	7.4(4)	0.35(3)	7.1(3)	0.37(3)	7.2(4)	0.33(3)	7.0(5)	0.32(4)	9.1(3)	0.280(15)
11	8.0(5)	0.23(2)	8.1(8)	0.20(3)	8.3(6)	0.19(2)	7.5(12)	0.18(5)	11.4(7)	0.148(12)

[a] Computed with RQMC using the CBS+corr potential for four CO isotopomers[22] and with the SAPT potential for the normal isotopomer.

this supports the view that the CBS+corr vibrational shift is too high in the size range $N \approx 30$ to 100.

B. Rotational Energy. The lowest rotational excitations of the cluster, as obtained[8,13] from the imaginary-time autocorrelation function of the molecular dipole, are displayed in Figure 3 for the $^{13}C^{18}O$ isotopomer; results for this and other isotopomers are collected in Tables 1 and 2, where a comparison is also made with results obtained using the SAPT potential for the normal isotopomer, $^{12}C^{16}O$. The well-known pattern[7,11−13,15] with two main series, named a-type and b-type after the corresponding spectral lines of dimer complex, is common to all isotopomers. For small N the a-type series has an end-over-end rotational character, low energy and weak spectral weight; as N increases, it gradually acquires free-rotor character and gains over 95% of the dipolar spectral weight. In the limit of large N the energy of the a-type series settles to the so-called nanodroplet value. Conversely, the b-type series, which originates from the free-rotor mode of the dimer, weakens and disappears for clusters of less than a dozen He atoms.

Experimentally, a limited number of split lines are observed, which show subtle differences among various isotopomers in the range $N = 4$ to 8.[7,12] In the presence of small line splittings, our procedure is not accurate enough to capture such fine details and presumably gives at best a weighted average of the split lines. This situation is further complicated, in the size range where the a-type and b-type series coexist, by the presence of two strong excitations which exhaust most of the oscillator strength. In this respect, the situation is more favorable for larger cluster sizes, where the b-type series has disappeared, and our spectral analysis is more robust. At $N = 15$, one further line splitting is seen in the experimental spectrum according to the so-called conventional numbering,[7] i.e., an assignment as consistent as possible with that of ref 11. However, different assignments in the size range around 15 cannot be excluded on

purely experimental grounds, and alternative numberings dubbed A, B, C, D are proposed in ref 7. These numberings produce a smoother evolution of the R(0) series (as well as a smoother dependence on isotopic substitution, see Section IIIC). This is shown in Figure 3 of ref 7, which compares the R(0) a-type series using either the conventional numbering or the D numbering with weighted average of split lines. This comparison is reported for convenience in Figure 3, after subtraction of the computed vibrational shift. The evolution of the a-type series with the D numbering is remarkably closer to the results of our simulations. In particular with the conventional numbering the experimental values have a gap between $N = 14$ and $N = 16$, significantly larger than the whole spread of the simulation data in the nearby size range (we do not consider here the two measured values assigned to $N = 15$, which would correspond to a single intermediate value after weighted average).

C. Isotopic Effect. The isotopic dependence on the measured R(0) transitions has been reported in ref 12 and 7 using the conventional numbering. A convenient picture of the effect is obtained by subtracting the origin of the vibrational band of individual isotopmers and taking the difference with the normal case, $^{12}C^{16}O$. Negative values are generally observed, due the increased reduced masses of $^{13}C^{16}O$, $^{12}C^{18}O$, and $^{13}C^{18}O$.

At small cluster sizes, the difference is relatively large for the b-type line, on account of its free-rotor character in the binary complex that reflects molecular properties. At larger sizes the difference decreases, corresponding to the increased solvent character of the rotational excitation of the cluster. Once again, for systems up to about 10 He atoms, fine details of split lines are beyond the accuracy of our calculation. The a-type line starts instead with negligible differences among isotopomers, corresponding to the initial end-over-end character of the series. Around a cluster size of a dozen He atoms, where the a-type series acquires a free-rotor character (see Figure 3 and ref 13), the difference increases, getting very close to its nanodroplet value already at $N = 20$. However the magnitude of the difference shows a pronounced dip precisely at $N = 15$ (in the conventional numbering). If one accepts the view that the line splitting at $N = 15$ is due to a near degeneracy with a He-related excitation,[13] this dip would merely reflect the increased mixing of solvent states in the cluster rotational state.

With any of the alternative numberings, either member of the former $N = 15$ doublet of the conventional numbering is paired to a different line with stronger spectral weight and stronger isotopic dependence. In the weighted average,[23] such a strong isotopic dependence prevails, and the dip in the difference weakens (for numberings A and B) or disappears (C and D).

Our results (see Figure 4 for the a-type series of the $^{13}C^{18}O$ isotopomer and Table 1 for a complete list) are in good agreement with the experiment, although we generally find a slight overestimate of the isotopic effect presumably due to the simplified treatment of the change in the He−CO potential mentioned in Section II. We note in particular the absence of a dip at $N = 15$ or $N = 16$. If one considers weighted averages for line doublets at given cluster size, this is consistent with numberings C, D but not with A, B or conventional.

The simulation results show instead a possible dip at $N = 17$ for $^{13}C^{18}O$. However this feature, not seen in the experimental data with any of the proposed[7] numberings, is rather weak and gets lost into the statistical error[24] for other isotopomers (see Table 1).

D. Approach of the a-Type Series to the Nanodroplet Regime. For the normal isotopomer, infrared spectra taken under conditions of maximum clustering show that individual R(0) transitions can be resolved up to $N \approx 50$, and provisional assignments are reported up to this size. The resulting a-type series is compared to simulation results[25] obtained with both CBS+corr and SAPT potentials in Figure 5. We note from Table 1 that the purely rotational energies are slightly higher with SAPT than with CBS+corr in the whole size range displayed in Figure 5. However, the stronger difference in the origin of the band (see Figure 1) prevails in the calculated R(0) transitions, with the SAPT results being too low. The documented quantitative accuracy of the CBS+corr PES for $N = 1$, the plausibility of the nearly linear behavior of the vibrational shift within the first solvation shell, and the excellent agreement between measured and calculated R(0) transitions up to $N \approx 30$, all support the high quality of the CBS+corr potential, at least for not too large He−CO distances. For $N = 30-100$, a better agreement would be obtained if the CBS+corr $\Delta\nu(N)$ decreased at a rate similar to the SAPT $\Delta\nu(N)$ in this range. In summary, (i) using the best currently available potential,[17] the calculated R(0) transitions are somewhat higher

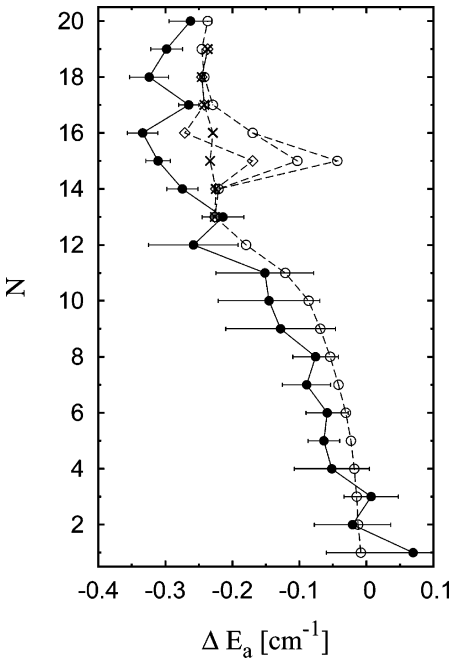

Figure 4. Difference between the a-type series of $^{13}C^{18}O@He_N$ and $^{12}C^{16}O@He_N$ clusters, after subtracting the respective monomer band origin: RQMC (filled circles), and experiment[7] with the conventional (open circles), B (open diamonds), and D (crosses) numberings. For B and D we have used weighted averages of split lines.[23]

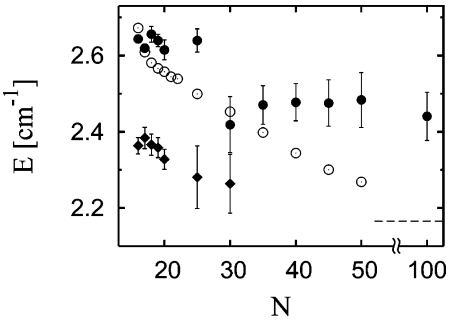

Figure 5. Detail of the a-type R(0) transitions in $^{12}C^{16}O@He_N$ for $N > 15$: RQMC results[25] with the CBS+corr (filled circles) and the SAPT (filled diamonds) potentials and experiment[7] (open circles);[26] the horizontal line is the nanodroplet value.[16] We have subtracted the origin of the vibrational band in the gas-phase.

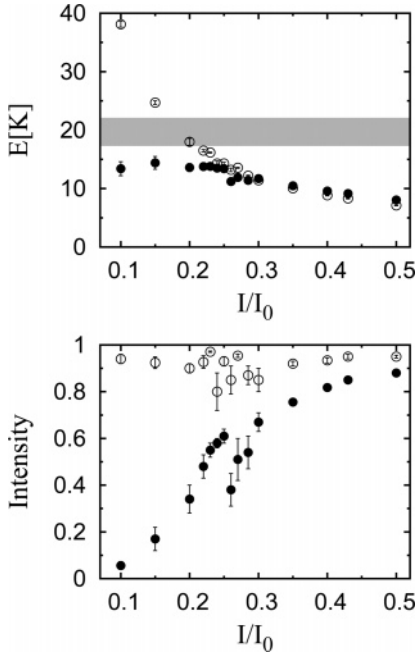

Figure 6. The lowest rotational energy (top panel) and its spectral weight (bottom panel) for fictitious molecular impurities solvated with 20 He atoms. These molecules have the same mass and the same interaction with He as the physical molecules (respectively CO (filled circles) and HCN (open circles)). Their moments of inertia, instead, are reduced with respect to the physical value by the factor I/I_0, as indicated by the abscissa. The shaded region encompasses the energy values (similar for both dopants and almost independent of I/I_0) of a He-related excitation of the cluster with angular momentum $J = 1$.

than their experimental values for large clusters; (ii) a comparative analysis with the SAPT potential, which is presumably more accurate at large He−CO distance, suggests that the vibrational shift, rather than the rotational energy, is too high (see Figure 1). Therefore, to attain its nanodroplet value, which is even higher, the vibrational shift must have a strong blue upturn at $N > 100$.

Because the R(0) lines measured for $N \approx 50$[7] and the nanodroplet limit[16] are already very close, a substantial blue upturn of the vibrational shift requires a corresponding decrease of the rotational constant. Indeed, the value given in ref 16 for the effective rotational constant (B_{eff}) in the nanodroplet limit is significantly smaller than that calculated previously[13,16] (see also Figure 3) in a wide range of cluster sizes between $N \approx 15$ and 100. The physical mechanism invoked in ref 16 to explain the lowering of B_{eff} in large droplets is the coupling of molecular rotation with He bulk-like phonons, which can have sufficiently low energies only at a low wave vector, or equivalently at a large system size. To simulate a somewhat similar physical effect with manageable system sizes, we artificially increase the gas-phase B value; the rotational energy thus eventually crosses a high-energy cluster excitation with angular momentum $J = 1$ involving mostly helium motions. The coupling of the molecular rotation with this mode is illustrated in Figure 6; the lowest rotational excitation of the cluster doped with CO is repelled by a solvent-related excitation, with a concurrent loss of spectral weight. Correspondingly, a second excitation (not shown for clarity), higher in energy than the He-related mode, gains weight and further shifts upward.

Interestingly, when we use HCN instead of CO as a dopant molecule, the molecular rotation is not significantly affected by a nearly degenerate He-related cluster excitation[13] (incidentally, this suggests that the splitting of the measured R(0) series close to $N = 15$ for CO@He$_N$ clusters[11] might not be observed in a similar experiment with HCN). This is consistent with the observation that the almost constant value of B_{eff}, predicted[10] between $N \approx 20$ and 50 for HCN@He$_N$, coincides with the measured nanodroplet value.[27]

The correlated basis function calculation of ref 16 explains this disparity between CO and HCN in terms of the different degree of anisotropy of the respective interaction potentials with He atoms. The present calculation gives support to this mechanism, but it does not have obvious implications on the displacement of the rotational excitation caused by the presence of a "quasi continuum" of states in the nanodroplet (which instead clearly affects the line shape[28]). Heading back to the R(0) transitions of real CO@He$_N$ clusters, the present results call for a demonstration that a sufficiently strong anisotropy can produce not only a reduction of B_{eff} but also a correspondingly large blue upturn of the vibrational shift, both in a range of N between hundreds and thousands.

IV. Conclusions

Using the recent CBS+corr potential[17] we have calculated the vibrational shift and rotational excitations of CO@He$_N$ clusters. The smoothness of the evolution of the resulting R(0) a-type series for all isotopomers studied favors the D numbering, one of the alternative assigments proposed by McKellar[7] in the size range around $N = 15$, over the conventional numbering of ref 11; further support is provided by the N dependence of the differences between isotopomers.

The general agreement between the calculated and measured R(0) series is very good, and it is somewhat better than that found using the SAPT potential of ref 20 (for small system size, see ref 22). For large cluster sizes ($N \approx 30-50$), it would further improve with ≈ 0.2 cm^{-1} more red shift of the origin of the vibrational band. Although the comparison with the size-selective measurements[7,11,12] is gratifying, the present results could be reconciled with the current estimate[16] for the nanodroplet limit only in the presence of a strong blue upturn for $N > 100$.

Acknowledgment. We thank G. Murdachaew and G. Scoles for useful discussions. We acknowledge the allocation of computer resources from the Iniziativa Calcolo Parallelo of the Italian Institute for the Physics of Matter (INFM).

References and Notes

(1) Choi, M. Y.; Douberly, G. E.; Falconer, T. M.; Lewis, W. K.; Lindsay, C. M.; Merritt, J. M.; Stiles, P. L.; Miller, R. E. *Int. Rev. Phys. Chem.* **2006**, *25*, 15−75.

(2) Toennies, J. P.; Vilesov, A. F. *Angew. Chem. Int. Ed.* **2004**, *43*, 2622−48.

(3) Stienkemeier, F.; Lehmann, K. K. *J. Phys. B* **2006**, *39*, R127−R166.

(4) Barranco, M.; Guardiola, R.; Hernández, S.; Mayol, R.; Navarro, J.; Pi, M. *J. Low Temp. Phys.* **2006**, *142*, 1.

(5) Tang, J.; Xu, Y. J.; McKellar, A. R. W.; Jäger, W. *Science* **2002**, *297*, 2030.

(6) McKellar, A. R. W.; Xu, Y.; Jäger, W. *Phys. Rev. Lett.* **2006**, *97*, 183401.

(7) McKellar, A. R. W. *J. Chem. Phys.* **2006**, *125*, 164328.

(8) Moroni, S.; Sarsa, A.;. Fantoni, S.; Schmidt, K. E.; Baroni, S. *Phys. Rev. Lett.* **2003**, *90*, 143401.

(9) Paesani, F.; Viel, A.; Gianturco, F. A.; Whaley, K. B. *Phys. Rev. Lett.* **2003**, *90*, 073401.

(10) Paolini, S.; Fantoni, S.; Moroni, S.; Baroni, S. *J. Chem. Phys.* **2005**, *123*, 114306.

(11) Tang, J.; McKellar, A. R. W. *J. Chem. Phys.* **2003**, *119*, 754.

(12) McKellar, A. R. W. *J. Chem. Phys.* **2004**, *121*, 6868.

(13) Cazzato, P.; Paolini, S.; Moroni, S.; Baroni, S. *J. Chem. Phys.* **2004**, *120*, 9071.

(14) Paesani, F.; Gianturco, F. A. *J. Chem. Phys.* **2002**, *116*, 10170.
(15) Zillich, R. E.; Paesani, F.; Kwon, Y.; Whaley, K. B. *J. Chem. Phys.* **2005**, *123*, 114301.
(16) von Haeften, K.; Rudolph, S.; Simanovski, I.; Havenith, M.; Zillich, R. E.; Whaley, K. B. *Phys. Rev. B* **2006**, *73*, 054502.
(17) Peterson, K.; and McBane, G. C. *J. Chem. Phys.* **2005**, *123*, 084314.
(18) Chuaqui, C. E.; Le Roy, R. J.; McKellar, A. R. W. *J. Chem. Phys.* **1994**, *101*, 39.
(19) Korona, T.; Williams, H. L.; Bukowski, R.; Jeziorski, B.; Szalewicz, K. *J. Chem. Phys.* **1997**, *106*, 5109.
(20) Heijmen, T. G. A.; Moszynski, R.; Wormer, P. E. S.; van der Avoird, A. *J. Chem. Phys.* **1997**, *107*, 9921.
(21) Baroni, S.; Moroni, S. *Phys. Rev. Lett.* **1999**, *82*, 4745.
(22) The results are unbiased in the limit of large projection time (β) and short time step (ϵ). Furthermore, for the given statistical precision, the accuracy of the inverse Laplace transform may depend on the interval (0, τ_{max}) of the computed imaginary-time correlation functions. In this work, the results pertaining to the CBS+corr potential are obtained with $\beta = 0.5$, $\epsilon = 10^{-3}$, and $\tau_{max} = 0.5\ K^{-1}$, which implies sampling paths with 1500 time slices. With this choice of τ_{max}, the rotational energies for small N are slightly overestimated. The SAPT results, obtained with $\tau_{max} = 0.7$ and $\epsilon = 5 \times 10^{-4}$, are better converged for small sizes.
(23) After Figure 2 of ref 7 (top trace) we have used weights in the ratios 87:125:17:36:50 for the lines assigned to 13, 14, 15a, 15b, and 16, respectively, in the conventional numbering.
(24) The error bars reported in the figures and the tables represent the statistical noise. The present results favor the D assignment under the assumption that other sources of bias (such as imperfections of the potential energy surface or the possible uncertainty related to the number of terms used to fit the imaginary-time correlation functions [ref 13]) have a sufficiently smooth dependence on N.
(25) The value at $N = 100$ has a somewhat uncertain statistical error, because it is obtained from simulations not much longer than the autocorrelation time of the random walk.
(26) In ref 7, the R(0) transitions of $^{12}C^{16}O@He_N$ assigned to $N = 26$, 30, 35, 40, 45, and 50 in Table II are labeled $N = 30$, 35, 40, 45, and 50 in Figures 4 and/or 5. Here, we use the numbering given in the figures, which follow the regular sequence mentioned [ref 7] in the text.
(27) Conjusteau, A.; Callegari, C.; Reinhard, I.; Lehmann, K. K.; Scoles, G. *J. Chem. Phys.* **2000**, *113*, 4840.
(28) Lehmann, K. K. *J. Chem. Phys.* **2007**, *126*, 024108.